Characterization of textile fibers by means of EGA-MS and Py-GC/MS

Authors

Tommaso Nacci[a]

[a] University of Pisa, Department of Chemistry and Industrial Chemistry

Via Giuseppe Moruzzi, 13, I-56124, Pisa (Italy)

nacci95@hotmail.it

Francesca Sabatini[a]

[a] University of Pisa, Department of Chemistry and Industrial Chemistry

Via Giuseppe Moruzzi, 13, I-56124, Pisa (Italy)

f.sabatini4@gmail.com

Claudia Cirrincione[b]

[b] Laboratorio di restauro arazzi e tappeti, Opificio Delle Pietre Dure (OPD), Ministero della Cultura

Sala delle bandiere, Palazzo Vecchio, Piazza della Signoria, I-50122, Firenze (Italy)

claudia.cirrincione@beniculturali.it

Ilaria Degano*[a,c]

[a] University of Pisa, Department of Chemistry and Industrial Chemistry

Via Giuseppe Moruzzi, 13, I-56124, Pisa (Italy)

[c] Center for Instrument Sharing of the University of Pisa (CISUP), University of Pisa, Italy

ilaria.degano@unipi.it (corresponding author)

Maria Perla Colombini[a]

[a] University of Pisa, Department of Chemistry and Industrial Chemistry

Via Giuseppe Moruzzi, 13, I-56124, Pisa (Italy)

maria.perla.colombini@unipi.it

Abstract

Textile fibers have represented an important resource for mankind throughout all human history. In fact, ancient cultures employed them not just to produce clothes, but also for expressing their habits and traditions. Based on the chemical composition, textile fibers are classified as natural, artificial, and synthetic. The analysis of textile fibers can be very challenging, so it is crucial to find new analytical tools capable of identifying them and studying their behavior in the environment. The collected information can be transferred in many different fields, such as the industrial sector, forensic science, environmental science, and heritage science.

In the present study, the capability of Pyrolysis coupled to Gas Chromatography and Mass Spectrometry (Py-GC/MS), and Evolved Gas Analysis coupled to Mass Spectrometry (EGA-MS) to discriminate textile fibers was tested. The first part of the study was addressed to the analysis of pure samples to build a detailed database by highlighting the main differences in the chromatographic profiles. Then, three textile blends of known composition were investigated, and the results compared with those acquired by Attenuated Total Reflectance Fourier Transform Infrared spectroscopy (ATR-FTIR). Eventually, the information obtained from the reference materials was exploited for the study of textile samples collected from the stage costumes of the lyrical opera 'I Puritani' directed by Franco Zeffirelli in 1961. The EGA-MS and Py-GC/MS results, integrated with those obtained by optical microscopy, allowed us to deepen the characterization of the historical samples.

Keywords

Textile fibers, historical textiles, Py-GC/MS, EGA-MS, ATR-FTIR, optical microscopy

1. Introduction

A textile fiber is a natural or man-made material used as the basic element of textiles and other woven fabrics [1]. Based on their chemical structure, textile fibers are classified as natural or man-made. Natural fibers are composed by polymers that occurs naturally (i.e., cellulose and proteins), while man-made fibers are the result of the processing of cellulose or synthetic polymers. Natural fibers can be either animal (e.g., silk and wool) or vegetal (e.g., cotton and flax).

Man-made fibers can be characterized either as artificial or synthetic. Artificial fibers are produced through direct or derivative methods. The former method requires the direct dissolution of cellulose in an appropriate solvent and the following spinning without any alteration in the cellulose chemical structure, and is employed to produce Bemberg, lyocell, modal, and viscose. In the latter method, instead, a derivatization step anticipates the dissolution. The cellulose derivative is then dissolved and spun before the fibers are regenerated (e.g., acetate). Conversely, synthetic fibers are obtained from raw materials such as petroleum-based chemicals (e.g., polyamides and polyesters) [2].

Fibers identification is an important task in many different fields, such as textile industry, fashion design, heritage science, and forensic science [3]–[6]. Microfibers are today recognized as a relevant pollutant for fresh and ocean waters, making their reliable and sensitive detection a hot topic in analytical and environmental research [7]–[10]. However, the analysis of textile fibers can be very challenging, and many considerations must be made to collect a representative sample. Natural fibers present an intrinsic variability that man-made fibers, especially the synthetic ones, do not have. In fact, man-made fibers are manufactured in controlled conditions, so there are not many variations between fibers of the same batch [11]. Another critical aspect is that many textiles are blends of different types of fibers or are woven with different types of yarns [12].

From the naked-eye observation of fibers physical appearance much information can be obtained, but the intrinsic micrometric diameter of most of the fibers makes examinations without magnification hard [11]. The use of microscopic techniques such as optical microscopy and Scanning Electron Microscopy (SEM) for the identification of natural and man-made fibers has been reported in literature [13]–[22]. Modern optical

and digital microscopes can provide high-resolution images by using magnifications of over x400, which enable the observation of objects in the micrometric dimensional range [23]–[25]. Microscopic methods represent to date the most reliable tool for the analysis of natural fibers, especially the vegetal ones [12], [14], [21]. The identification of textile fibers must involve the comparison with reference fibers to ensure the validation of the procedure [12], [26]. Unfortunately, no online database for the fibers globally produced is currently available, so it is necessary to collect reference materials (e.g., plants and animal hairs) from the study regions [19], [27], [28]. In addition, biology knowledge and a high level of skills are crucial to distinguish fibers from other types of cells [11], [12], [14], [21], [26].

Nowadays, infrared and Raman spectroscopies are widely employed in forensic science due to their non-destructive nature, preventing any alteration of the sample, which constitutes official evidence [29]–[35]. Fourier Transform Infrared spectroscopy (FTIR) is one of the most common techniques for investigating synthetic fibers because the polymeric matrix shows a significant absorption in the spectral range between 1800-1000 cm^{-1} [36], [37]. Recent works have demonstrated that Attenuated Total Reflectance FTIR spectroscopy (ATR-FTIR) allows the classification of textile blends as well [38]. However, Raman spectroscopy revealed a major capability to distinguish the fibers subclasses compared to ATR-FTIR spectroscopy, except for acrylics fibers [39], [40]. Although spectroscopic techniques are considered the election method for the analysis of synthetic fibers, they struggle to discriminate cellulose-based fibers, preventing the exhaustive characterization of the samples [41], [42].

Thus, destructive techniques shall be employed, which provide more detailed information on the fiber itself and on dyes and additives possibly present [43]–[45]. High Performance Liquid Chromatography coupled to Mass Spectrometry (HPLC-MS) is a promising technique to be applied due to its great separation efficiency, that permits to resolve the components of very complex mixtures, and the great sensitivity [46]–[48]. Nevertheless, this approach entails the alteration of the fiber structure by wet chemical treatments [43]. Multi-Shot Pyrolysis coupled to Gas Chromatography and Mass Spectrometry (Py-GC/MS), and Evolved Gas Analysis coupled to Mass Spectrometry (EGA-MS) are promising techniques that have provided useful information in the analysis of wool fibers [49]. Unfortunately, the application of Py-GC/MS and EGA-MS to

the analysis of other natural and manufactured textile fibers is still limited due in part to their recent development and the challenging interpretation of the results, especially when dealing with natural fibers [50]–[52]. Another critical issue is the lack of optimized and standardized methods for the identification and quantification of microfibers [53].

In this paper, we present a study on textile fibers based on Py-GC/MS and EGA-MS. We aim at building a detailed database of the most common natural, artificial, and synthetic textile fibers and find characteristic m/z ions and pyrolytic markers allowing the identification of unknown samples. The variability due to the manufacturing process were also evaluated by analyzing three samples of cotton, viscose, and polyester from different manufacturers. In addition, three textile blends of known composition were analyzed by ATR-FTIR, EGA-MS and Py-GC/MS to highlight the main advantages and limitations of each approach.

A case study is presented to prove the potentialities of the technique, dealing with the investigation of 20th century stage costumes, which are expected to contain complex mixtures of natural, artificial, and synthetic fibers. All the samples were preliminary observed under Optical Microscope (OM). The need to minimize sample size and the possible occurrence of degradation of the textiles make the application of sensitive techniques particularly appropriate in this field. In detail, the reference database was used to characterize the composition of yarn samples collected from the stage costumes of the lyrical opera 'I Puritani' directed by Franco Zeffirelli in 1961.

2. Materials and methods

2.1 Reference materials

A set of reference textile materials, including fabrics made of the most common natural (both animal and vegetal), artificial and synthetic fibers, was investigated (Table 1). The set mostly consisted of pure samples, but also included three textile blends of known composition. Some of the samples were provided by the Tapestries and Carpets and Textiles Laboratory of the restoration center *Opificio delle Pietre Dure di Firenze* (OPD, Florence, Italy) while others were bought as swatches on an online shop (www.tessuti.com).

2.2 Historical samples

Twelve yarns samples from the stage costumes of the lyrical opera 'I Puritani' directed by Franco Zeffirelli in 1961 were analyzed (**Figure *1*:** Stereomicroscopy images of samples A_01 (A), A_02 (B), A_03 (C), A_04 (D), E_01 (E), E_02 (F), E_03 (G), E_04 (H), E_05 (I), E_06 (L), E_07 (M), and E_08 (N).Figure 1). The costumes were designed by Peter Hall and manufactured by the tailoring shop of the Teatro Massimo in Palermo (*Sartoria del Teatro Massimo di Palermo*). Today they belong to the Foundation Teatro Massimo of Palermo (*Fondazione Teatro Massimo di Palermo*). The samples were collected from the stage costumes of the two main characters of the opera, Arturo and Elvira, and were kindly provided by the restorer Claudia Cirrincione (OPD, Florence, Italy) [54]. Samples A_01 and A_02 were collected from Arturo's jacket, A_03 and A_04 from Arturo's cloak. Sample A_01 was the only coloured sample, and dye analysis detected markers of Diamond Green G (CI 42040, Basic Green 1) [55]. Samples from Elvira's dress were collected from the over skirt and bodice (E_01, E_02), the stomacher (E_03), the skirt (E_04), the train (E_05, E_06), the petticoat (E_07), and finally from the bodice (E_08).

Table 1: Set of reference samples.

Sample	Composition	Origin
Cotton #1	Cellulose	Online shop
Cotton #2	Cellulose	Online shop
Cotton #3	Cellulose	Online shop
Flax	Cellulose	Online shop
Jute	Cellulose	Online shop
Silk	Proteins	Online shop
Wool	Proteins	OPD
Acetate	Acetylated cellulose	Online shop
Bemberg	Regenerated cellulose	Online shop
Lyocell	Regenerated cellulose	Online shop
Modal	Regenerated cellulose	Online shop
Viscose #1	Regenerated cellulose	OPD
Viscose #2	Regenerated cellulose	Online shop
Viscose #3	Regenerated cellulose	Online shop
Acrylic	Polyacrylonitrile (PAN)	Online shop
Polyamide	Nylon 6	Online shop
Polyester #1	Poly(ethylene terephthalate) (PET)	OPD
Polyester #2	Poly(ethylene terephthalate) (PET)	Online shop
Polyester #3	Poly(ethylene terephthalate) (PET)	Online shop
Polyvinyl alcohol (PVA)	Polyvinyl alcohol (PVA)	Online shop
Polyvinyl chloride (PVC)	Polyvinyl chloride (PVC)	Online shop
50% acrylic 50% wool	PAN and proteins	OPD
60% polyester 40% polyamide	Polyester and Nylon 6	OPD
92% acrylic 8% polyamide	PAN and Nylon 6	OPD

2.3 Methods

2.3.1 EGA-MS

The instrumentation consisted of a Multi-Shot Pyrolyzer EGA/Py-3030D microfurnace (Frontier Laboratories Ltd. Fukushima, JP) coupled to a 6890N Gas Chromatograph (Agilent Technologies, Palo Alto, USA). A deactivated and uncoated stainless-steel transfer tube (UADTM-2.5 N, 0.15 mm i.d. x 2.5 m length, Frontier Lab) was used to connect the injection port and the mass spectrometer. The products evolved from the samples over the temperature range were transferred to the mass spectrometer, ionized, and analyzed as a function of time. The detector was an Agilent 5973 Mass Selective Detector (Palo Alto, USA) single quadrupole mass spectrometer operating in electron ionization mode (EI) at 70 eV, in positive mode scanning in the range from 35 to 600 m/z. The MS source was kept at 230 °C and the MS quadrupole at 150 °C.

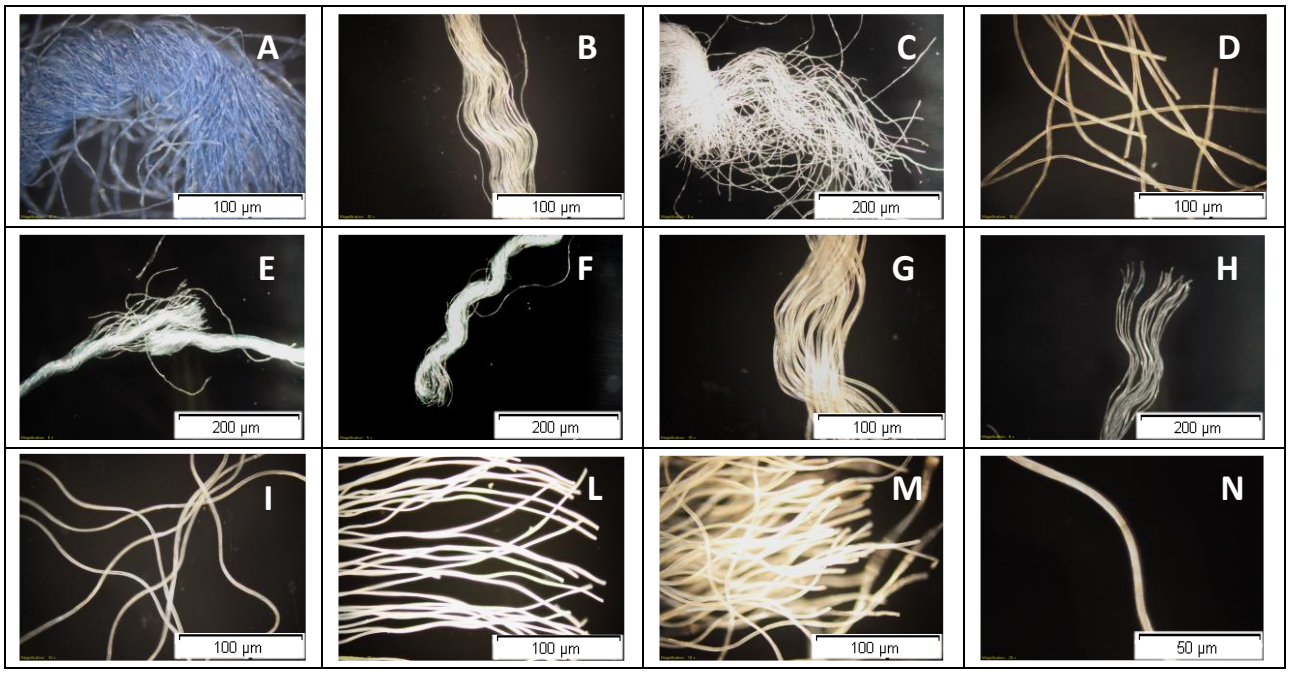

Figure 1: Stereomicroscopy images of samples A_01 (A), A_02 (B), A_03 (C), A_04 (D), E_01 (E), E_02 (F), E_03 (G), E_04 (H), E_05 (I), E_06 (L), E_07 (M), and E_08 (N).

About 300 µg of each sample were placed into a clean stainless-steel cup and inserted into the microfurnace. The temperature program chosen for the microfurnace was: initial temperature 50 °C then 10 °C/min up to 800 °C. The interface temperature was kept 100 °C higher than the furnace temperature up to 300 °C. The injection port operated at 280 °C, with a 1:20 split ratio. The chromatographic oven was kept at 300 °C during the whole EGA analysis. The analyses were performed in constant flow mode at 1.0 mL/min (He, purity 99.995%). The data collected were processed by Agilent MSD ChemStation (version D.02.00.275).

The reproducibility of the method was evaluated by analyzing the sample of viscose #1 in triplicate and calculating the relative standard deviation (RSD) of the normalized area of the Total Ion Thermogram (TIT). Normalized area was obtained from the integral in the 20-45 min interval of the TIT, divided by the sample weight. The sample of viscose was chosen because of its intermediate characteristics between natural and synthetic fibers. In fact, although it is a cellulose-based fiber, it requires a quite complex manufacturing process [56]. The technique showed an intra- and inter-day reproducibility of 3% and 10%, respectively.

The variability of the peak temperature (T_p), defined as the temperature corresponding to the maximum of the TIT profile, was evaluated for all the inter-day replicates of viscose #1 by t-test. A difference of the T_p lower than 3 °C resulted not statistically significant at 95% confidence level.

2.3.2 Py-GC/MS

The instrumentation used for Py-GC/MS was the same used for EGA-MS. However, the transfer tube was replaced by a deactivated silica pre-column (2 m x 0.32 mm i.d., Agilent J&W, USA) and an HP-5MS fused silica capillary column (stationary phase 5% diphenyl-95% dimethyl-polysiloxane, 30 m x 0.25 mm i.d., 0.25 μm Hewlett Packard, USA). About 90 μg of each sample were placed into a clean stainless-steel cup, inserted into the micro-furnace and pyrolyzed. All pure reference samples were pyrolyzed at 600 °C following the instrumental parameters reported in literature for the analysis of synthetic polymers [57]. The pyrolysis temperatures adopted for the textile blends and the historical samples were chosen based on the thermal regions showed by the EGA profiles of each sample. Thus, it was possible to characterize each thermal region separately, enhancing the discrimination capability of the technique. Where the EGA profile showed only one thermal region, the sample was pyrolyzed at 600 °C like the reference ones to simplify the comparison with the pyrograms in the database. The injection port operated at 280 °C, with 1:10 split ratio, and the interface temperature was kept at 280 °C. The pyrolysis products were eluted in constant flow mode at 1.2 mL/min (carrier gas He, purity 99.995%); the chromatographic program was: initial temperature 40 °C for 5 min, 10 °C/min to 310 °C for 20 min. The operating conditions of the mass spectrometer were the same ones adopted for EGA-MS analysis. The data collected were processed by AMDIS (version 2.62) and the NIST Mass Spectral Search Program (version 2.0). The reproducibility of the method was evaluated by analyzing the sample of

viscose #1 in triplicate and calculating the relative standard deviation (RSD) of the area of levoglucosan peak in the Total Ion Chromatogram (TIC) normalized towards sample weight. The technique showed an intraday reproducibility of 8%.

2.3.3 ATR-FTIR

The instrumentation consisted of a Perkin-Elmer Spectrum GX FT-IR equipped with a MIRacle^{TM} ATR. Each textile blend was analyzed using a germanium crystal (penetration of the radiation around 0.66 µm). Sixteen scans were collected from 4000 to 660 cm^{-1} with a resolution of 4 cm^{-1}. The spectra were acquired by Spectrum software (version 3.02) and processed with Jasco Spectra Manager software (version 1.53.04).

2.3.4 Optical microscopy

The instrumentation consisted in a Zeiss optical microscope, model AXIO Imager.A1 with Zeiss objective lens EC Epiplan-Neofluar 10x (0.25 HD), 20x (0.5 HD) and 40x. Fiber's longitudinal shape were observed under visible transmitted light at 10x, 20x and 40x magnifications. The images were acquired by Zeiss Zen Software. The analyses were carried out at the Scientific Laboratory of the OPD.

3. Results and discussion

3.1 Reference materials

3.1.1 EGA-MS

The peak temperatures (T_p) of the pure samples were obtained from TITs as the temperatures corresponding to the maxima of the EGA profiles and reported in Figure 2 to ease the comparison. Each fiber was analyzed in triplicate and the corresponding T_p was calculated as the average value. Whenever the EGA profile showed more thermal regions, only the T_p of the region at the highest temperature is reported for the sake of comparison. All the TITs and the corresponding average mass spectra of the pure samples are reported in Table S1 in Supplementary data. Synthetic fibers are the only ones showing T_p higher than 400 °C. Animal fibers are less thermally stable than cellulose-based fibers, featuring T_p ranging between 330 and 340 °C. Bemberg fibers showed the lowest T_p compared to all the other ones, probably due to the presence of traces

of copper that catalyze the degradation of cellulose, as observed in the literature [58]. Furthermore, vegetal fibers have a better thermal stability than artificial ones with T_p around 367-370 °C.

Vegetal and regenerated fibers present high relative abundances of ions at m/z 60 and 73 in their average mass spectra, attributable to anhydro sugars generated during the pyrolysis of cellulose-based substrates [59]. Acetate fibers pose the only exceptions, featuring m/z 43 and 81 as the main ions in their average spectra, corresponding to acetic acid and triacetate anhydro sugars [57]. However, ions at m/z 43 and 60 are featured in the average mass spectra of all cellulose-based fibers and PVA, so they cannot be used as marker ions. Conversely, the average mass spectra of animal fibers are characterized by ions at m/z 70 and 154, which correspond to 2,5-diketopyperazines (DKPs) [49]. The formation of DKPs is a characteristic process of proteinaceous substrates caused by the cyclization of proximal amino acid residues in the polypeptide chain [60].

Regarding synthetic fibers, ions at m/z 55 and 113, corresponding to ε-caprolactam, are typical of nylon 6 fibers [61], while ions at m/z 66 and 106, assigned to unsaturated nitriles, are representative of acrylic fibers [57]. Finally, polyester fibers show an average mass spectrum dominated by ions at m/z 105 and 149, corresponding to phthalates [62], which are a class of plasticizers commonly employed as additives in the manufacturing of textiles [63].

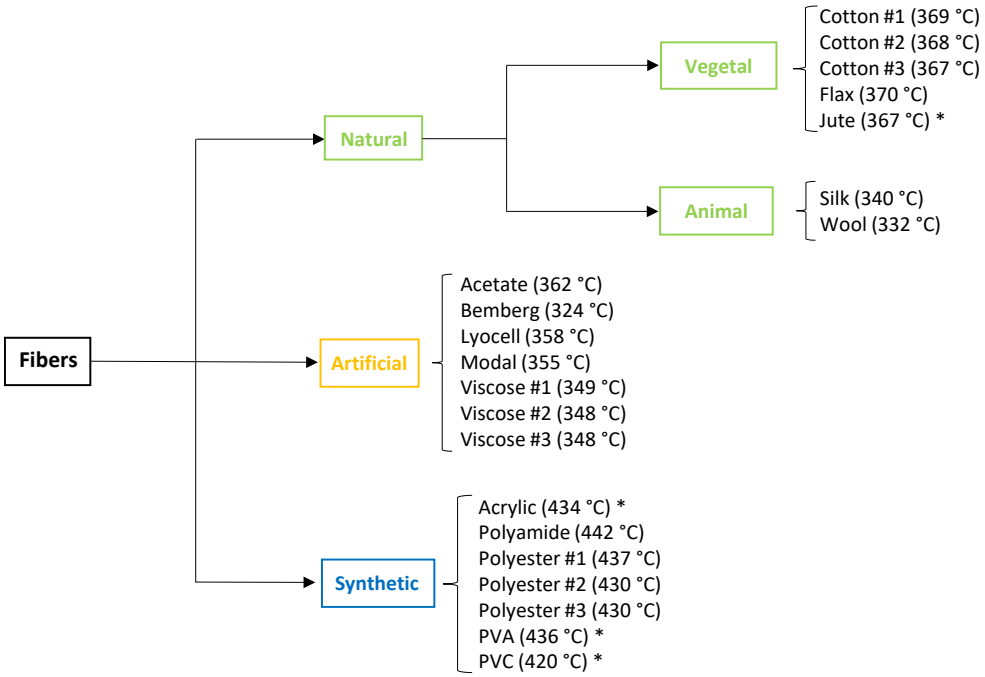

Figure 2: Peak temperatures (T_p) obtained from the TITs of all pure samples. * = the TIT of the sample featured more than one thermal degradation step. The TITs and the corresponding average mass spectra of the samples are reported in Table S1 in Supplementary data.

The effects due to manufacturing were also considered. Figure 3 shows the normalized TITs of samples of specimens of cotton, viscose, and polyester produced from different manufacturers. The TITs of the three cotton samples have a maximum at 348 °C but differ from each other at temperatures higher than 370 °C where the gases evolved from cotton #2 are less abundant compared to those evolved from cotton #1 and cotton #3. In addition, the TIT of cotton #3 presents a shoulder around 470 °C. The major difference between the average mass spectra of these samples lies between 35 and 70 m/z. In particular, the average mass spectra of cotton #1 and cotton #3 feature a high relative abundance of the ions at m/z 43 and 60 while cotton #2 has an average mass spectrum with 44 m/z as base peak. This is probably due to the great variability in the composition of natural fibers, which depends on many factors such as the cultivation parameters (e.g., plant species, soil, weather, use of pesticides) and the manufacturing process (e.g., fibers extraction, chemicals, dyes) [64].

The thermogram of viscose #2 features a shoulder in the thermal region between 300 and 340 °C while a higher abundance of gases is evolved from viscose #1 at temperatures higher than 350 °C. However, the average mass spectra of the viscose samples show the same pattern.

Although the thermograms of the three polyester samples are very similar, polyester #1 has a T_p statistically significantly higher compared to the other two. In addition, the average mass spectrum of polyester #1 presents lower relative abundance of the ions at m/z 44 and 149. This behavior suggests that the sample of polyester #1 contains a lower concentration of phthalates. In fact, many phthalates evolve at temperatures lower than 400 °C, resulting in a lower T_p.

Summarizing, the evaluation of TIT profiles and the corresponding average mass spectra obtained by EGA-MS highlighted the greater variability of the response of a natural fiber like cotton compared to man-made fibers, such as viscose and polyester.

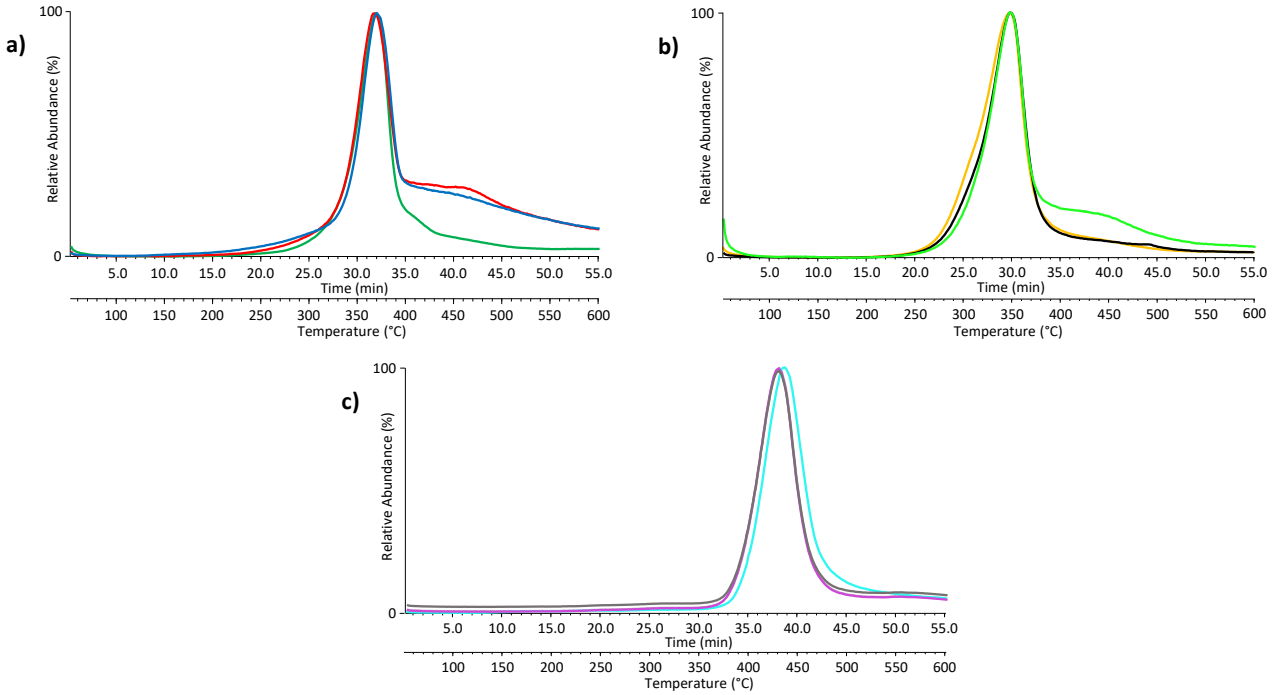

Figure 3: Normalized TITs of a) cotton #1 (blue), cotton #2 (green) and cotton #3 (red); b) viscose #1 (green), viscose #2 (orange) and viscose #3 (black); c) polyester #1 (light blue), polyester #2 (grey) and polyester #3 (purple). The average mass spectra of the samples are reported in Table S1 in Supplementary data.

3.1.2 Py-GC/MS

The results obtained by Py-GC/MS agree with those obtained by EGA. The pyrograms of all natural and artificial samples are shown in Figures S1 and S2 in Supplementary data and the peaks identification is reported in Tables S2 and S3 in Supplementary data. The Py-GC/MS chromatogram of wool was already reported and discussed in the literature [49], so it is not shown. The following considerations on natural and artificial fibers can be drawn:

- the pyrolytic profiles of all the vegetal fibers feature 1,4:3,6-dianhydro-α-D-glucopyranose and levoglucosan, typical pyrolysis products of cellulose or cellulose-based materials. In particular, levoglucosan is an anhydro sugar produced, together with its isomers galactosan and mannosan, when cellulose and hemicelluloses are pyrolyzed at temperatures above 300 °C [59]. 1,4:3,6-dianhydro-α-D-glucopyranose and levoglucosan are also detected in the pyrograms of artificial fibers, with the notable exception of acetate;
- the pyrograms of acetate fibers show a characteristic, very broad and particularly intense, peak due to acetic acid, and several acetylated anhydrosugars, such as 1,3,4,6-tetra-O-acetyl-β-D-glucopyranose;
- as expected, silk and wool are the only natural fibers which do not present any anhydro sugar related peak in the pyrogram. Their pyrolytic profiles feature nitrogen-containing heterocyclic compounds, such as cyclo(Pro-Ile) and cyclo(Pro-Hyp). In addition, their pyrograms showed phenol and 4-methyl-phenol as main pyrolysis products.

More specifically, for natural and regenerated fibers it is not possible to establish any pyrolysis marker enabling us to determine their specific type. Therefore, Py-GC/MS can only point to the general composition of cellulose fibers, whereas anatomical identification by microscopy observation remains the most reliable way to discriminate and identify them [50]. The identification of synthetic fibers is an easier task, compared to natural and artificial ones. Pyrolysis of synthetic polymers has also already been discussed and reported in the literature, and dedicated atlas are also available [57], [65]. Peaks assignment for the pyrograms of synthetic fibers are reported in Table S4 in Supplementary data and the main results are summarized as follows:

- the markers of acrylic fibers are nitriles, produced by rearrangements and cleavage reactions of the main polymeric structure [57];
- regarding polyamide fibers, ε-caprolactam is the main pyrolysis product for Nylon 6 and can be used as identifier to establish the chemical nature of a polyamide. In addition, a series of mononitrile compounds containing an amide group is detected. These species differ from each other for the length of aliphatic chain and, in some cases, for the saturation degree [57];

- polyester fibers pyrograms are dominated by aromatic species, such as terephthalates. In particular, divinyl benzoate is an identifier for PET [66];
- PVC features aromatic and chlorinated compounds as markers [57];
- PVA presents pyrolytic markers probably obtained from oxidation and rearrangement of the polymeric chain [67].

Table 2 summarizes the characteristic ions and pyrolysis markers established by EGA-MS and Py-GC/MS for all the samples.

Table 2: Characteristic m/z ions and pyrolysis markers established by EGA-MS and Py-GC/MS for all the samples.

Fiber	Characteristic ions (m/z)	Pyrolytic markers
Vegetal and regenerated	60, 73 (anhydro sugars)	1,4:3,6-dianhydro-α-D-glucopyranose Levoglucosan
Acetate	43, 81 (acetic acid and triacetate anhydro sugars)	1,3,4,6-tetra-O-acetyl-β-D-glucopyranose
Silk and wool	70, 154 (DKPs)	Phenol 4-methyl-phenol Cyclo (Pro-Ile) Cyclo(Pro-Hyp) Cyclo(Pro-Ala) Diketopyrrole Cyclo(Pro-Val)1&2
Acrylic	66, 106 (unsaturated nitriles)	Methacrylonitrile 2,4-pentadienenitrile 2-methylene-butanenitrile Hex-5-ene-1,3,5-tricarbonitrile (trimer) Hexane-1,3,5-tricarbonitrile (trimer) Pentane-1,3,5-tricarbonitrile (trimer) Hex-1-ene-1,3,5-tricarbonitrile (trimer)
Polyamide (Nylon 6)	55, 113 (ε-caprolactam)	Caprolactone ε-caprolactam N-(5-cyanopentyl)acetamide N-(5-cyanopentyl)butyramide N-(5-cyanopentyl)pent-4-enamide N-(5-cyanopentyl)pentanamide N-(5-cyanopentyl)hex-5-enamide N-(5-cyanopentyl)hexanamide
Polyester (PET)	105, 149 (phthalates)	Benzeneacetaldehyde Vinyl benzoate 4-ethylbenzoic acid Vinyl trans-cinnamate Divinyl terephthalate 4-(vinyloxycarbonyl)benzoic acid 1,2-ethanediol dibenzoate 2-(benzoyloxy)ethyl vinyl terephthalate
PVA		4-penten-2-one 1-methyl-cyclohexa-1,3-diene Acenaphthylene
PVC		1,4-dichlorobutane Benzene 2-methyl-1-hexene Toluene 3-methylene-heptane 3-(chloromethyl)-heptane 2-ethyl-1-hexanol Naphthalene

3.2 Textile blends

For the textile blends, the results obtained by the three analytical techniques are discussed in the following paragraphs presenting advantages and disadvantages of each one.

3.2.1 ATR-FTIR

The identification of the observed ATR-FTIR bands for all the three samples is reported in **Table *3*:** Vibrational mode assignment for the ATR-FTIR spectra of the samples composed of 50% acrylic and 50% wool (Figure *4*a), 60% polyester and 40% polyamide (Figure *4*b), and 92% acrylic and 8% polyamide (Figure *4*c).Table 3 [9], [36], [38]. The C≡N stretching band (2239 cm^{-1}) in the ATR-FTIR spectrum of the sample composed of 50% acrylic and 50% wool (Figure 4a) confirms the presence of acrylic fibers while most of the other spectral signals derive from the protein fraction. In particular, the amide I (1645 cm^{-1}) and amide II (1520 cm^{-1}) bands are characteristic of proteins. The C=O stretching band (1738 cm^{-1}) is typically related to comonomers used in the PAN synthesis [37].

The ATR-FTIR spectrum of the sample composed of 60% polyester and 40% polyamide (Figure 4b) shows bands due to the C-C(=O)-O (1250 cm^{-1}) and O-C-C (1103 cm^{-1}) stretching vibrations characteristic of the polyester fraction, whereas it does not feature any signal that can be exclusively assigned to the polyamide fraction. In addition, it is not possible to identify the specific type of polyester.

The spectral signals in the ATR-FTIR spectrum of the sample composed of 92% acrylic and 8% polyamide (Figure 4c) have a very low signal to noise ratio, and the spectrum presents a spectral region at wavelength higher than 3500 cm^{-1} with relevant spectral noise. This may be due to the diameter of acrylic and polyamide fibers, which is of the same order of magnitude as the wavelength of the incident light. However, it is possible to discriminate the C≡N (2241 cm^{-1}) and C=O (1726 cm^{-1}) stretching bands due to the acrylic and polyamide fraction, respectively. As for the previous sample, it is impossible to identify the type of polyamide used in the blend.

The results highlight the limitations of ATR-FTIR in the assignment of the minor components in the fibers, whenever a textile blend is analyzed.

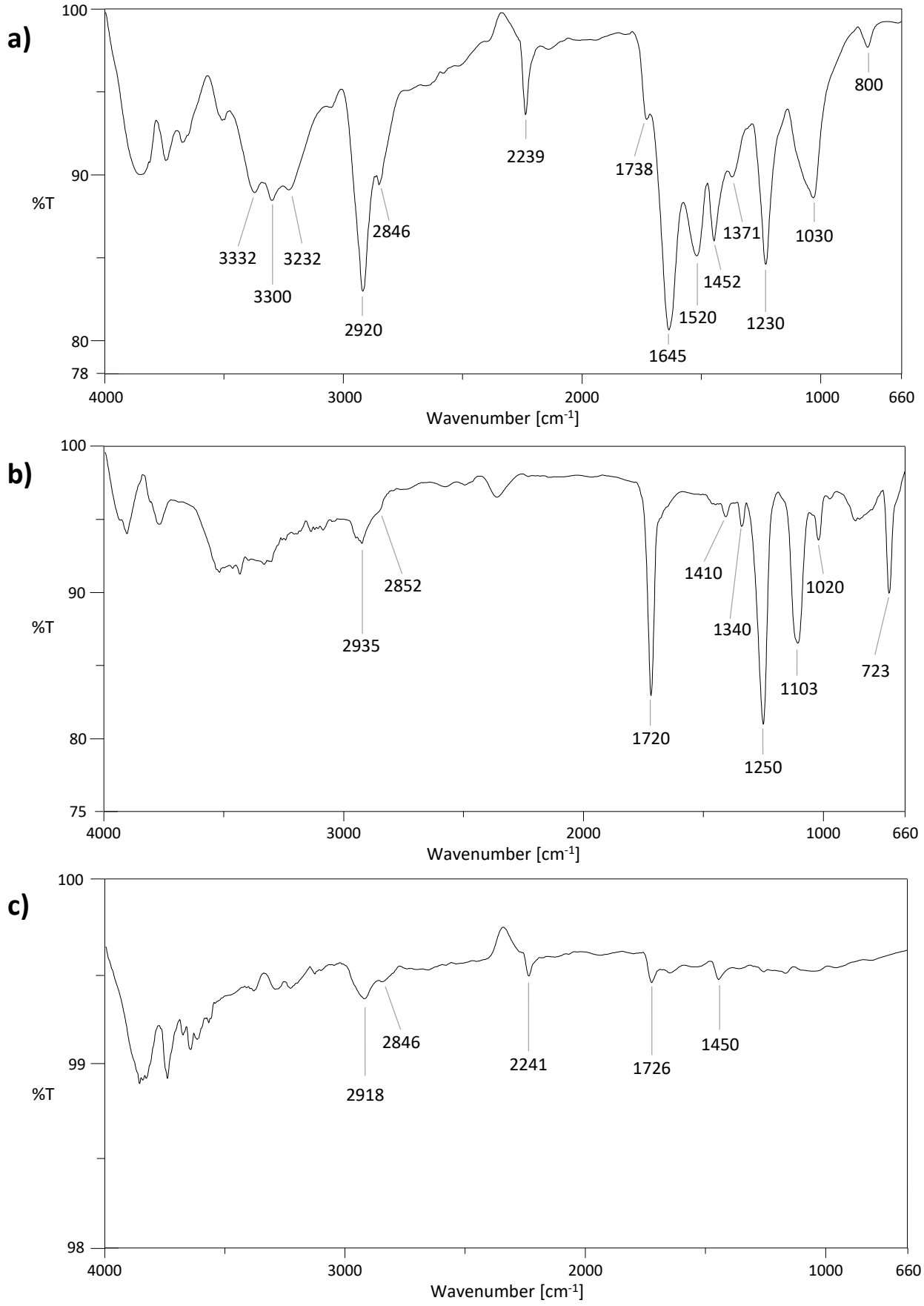

Figure 4: ATR-FTIR spectra obtained for the samples composed of a) 50% acrylic and 50% wool, b) 60% polyester and 40% polyamide, and c) 92% acrylic and 8% polyamide. Band assignments are reported in Table 3.

Table 3: Vibrational mode assignment for the ATR-FTIR spectra of the samples composed of 50% acrylic and 50% wool (Figure 4a), 60% polyester and 40% polyamide (Figure 4b), and 92% acrylic and 8% polyamide (Figure 4c).

Sample	Wavelength (cm^{-1})	Assignment
50% acrylic 50% wool	3332, 3300, 3232	N-H / O-H stretching
	2920	C-H_2 asymmetric stretching
	2846	C-H_2 symmetric stretching
	2239	C≡N stretching
	1738	C=O stretching
	1645	Amide I band
	1520	Amide II band
	1452	C-H_2 scissoring
	1371	C-H_2 twisting
	1230	N-H bending / C-N stretching
	1030	C-O stretching
	800	N-H wagging
60% polyester 40% polyamide	2935	C-H_2 asymmetric stretching
	2852	C-H_2 symmetric stretching
	1720	C=O stretching
	1410	C=C stretching
	1340	C-H_2 twisting
	1250	C-C(=O)-O stretching
	1120	O-C-C asymmetric stretching
	1103	O-C-C symmetric stretching
	1020	C-O stretching
	723	C-H_2 rocking
92% acrylic 8% polyamide	2918	C-H_2 asymmetric stretching
	2846	C-H_2 symmetric stretching
	2241	C≡N stretching
	1726	C=O stretching
	1450	C-H_2 scissoring

3.2.2 EGA-MS

The TIT curve of the blend composed of 50% acrylic and 50% wool (Figure 5a) presents a maximum (peak temperature, T_p) at 322 °C, a lower temperature compared to both T_p of the components. Ions at m/z 66, 106, 70, and 154 in the average mass spectrum (Figure 5b) confirms the capability of the technique to discriminate the components. The evaluation of the Extracted Ion Thermograms (EITs) allowed us to assign the main EGA peak to the acrylic component, while wool markers are evolved in correspondence to the shoulder around 270 °C.

The TIT curve of the blend composed of 60% polyester and 40% polyamide (Figure 6a) presents a maximum at 403 °C, a lower temperature compared to the T_p of both the components. The detection of high relative abundance of ions at m/z 55, 113, 105, and 149 in the average mass spectrum (Figure 6b) identifies the two fractions. Even if the TIT showed a single curve, by inspecting the EITs it is possible to clearly distinguish the polyamide component, which dominates the thermal region at temperatures below 410 °C, from the polyester one, which dominates the thermal region at temperatures above 410 °C.

The TIT curve of the blend composed of 92% acrylic and 8% polyamide (Figure 7a) presents two thermal regions, with maxima at 333 °C and 441 °C, roughly corresponding to the T_p of the pure acrylic sample. In fact, the TIT profile of acrylic fiber features two thermal regions with maxima at 318 °C and 433 °C. The average mass spectrum (Figure 7b) features ions mainly attributable to the acrylic components. Only the ion at m/z 113 was extracted for the evaluation of the polyamide fraction since the ion at m/z 55 is also one of the main ions in the acrylic mass spectrum. It was impossible to assign the gases evolved in any thermal region to the polyamide fraction of the blend, probably due to the low percentage of this component in the sample.

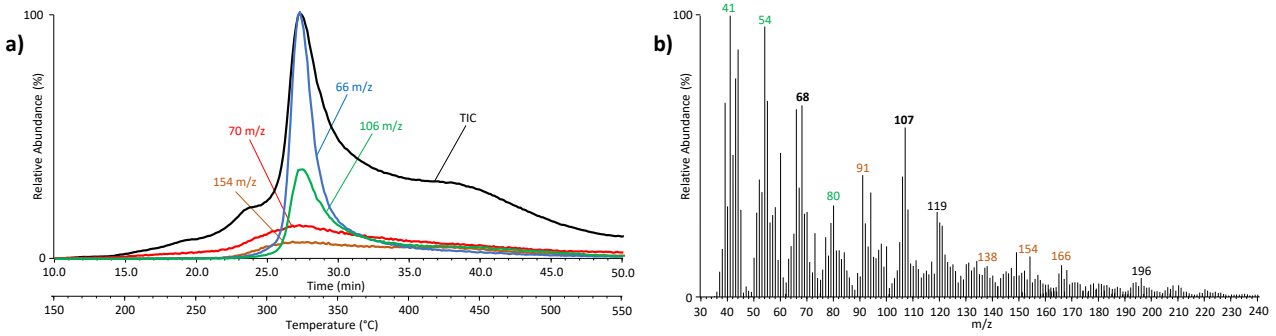

Figure 5: a) TIT and EITs of ions at m/z 66, 106, corresponding to unsaturated nitriles, and m/z 70, 154, corresponding to 2,5-diketopiperazines, of the sample composed of 50% acrylic and 50% wool; b) Average mass spectrum obtained from the TIT (20-45 min, 250-500 °C) of the sample composed of 50% acrylic and 50% wool. The characteristic ions of acrylic fibers are highlighted in green, those of wool fibers in brown and the ions in common to both components in bold.

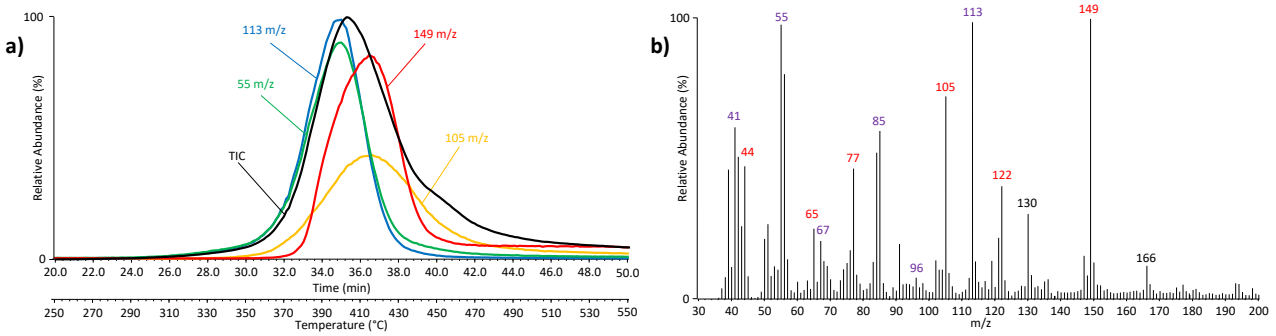

Figure 6: a) TIT and EITs of ions at m/z 55, 113, corresponding to ε-caprolactam, and m/z 105, 149, corresponding to phthalates, of the sample composed of 60% polyester and 40% polyamide; b) Average mass spectrum obtained from the TIT (30-45 min, 350-500 °C) of the sample composed of 60% polyester and 40% polyamide. The characteristic ions of polyester fibers are highlighted in red while those of polyamide fibers in purple.

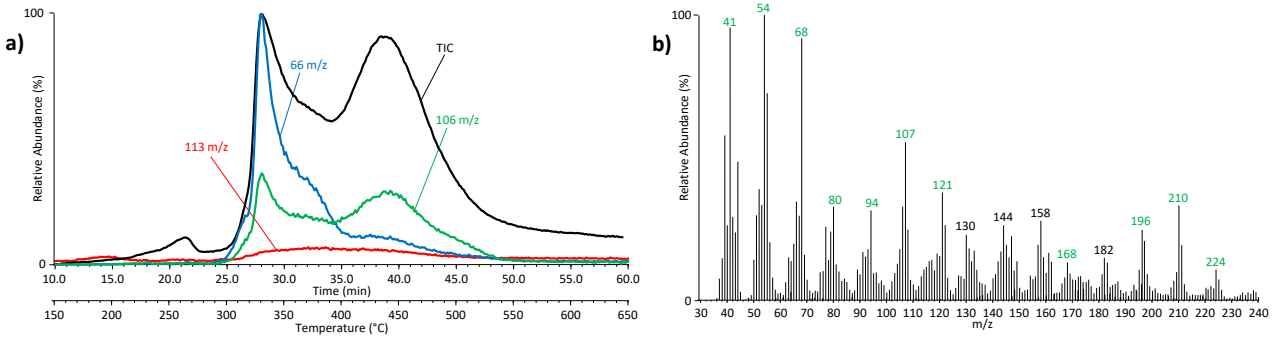

Figure 7: a) TIT and EITs of ions at m/z 66, 106, which correspond to unsaturated nitriles, m/z 113, which correspond to ε-caprolactam, of the sample composed of 92% acrylic and 8% polyamide; b) Average mass spectrum obtained from the TIT (25-55 min, 300-600 °C) of the sample composed of 92% acrylic and 8% polyamide. The characteristic ions of acrylic fibers are highlighted in green.

3.2.3 Py-GC/MS

It is important to highlight that semi-quantitative results are not easy to be obtained by Py-GC/MS, due to the possible occurrence of synergistic effects in the pyrolysis process [68]. Nonetheless, the technique proved able to detect both major and minor components in the fibers, as reported below.

The pyrogram obtained at 600 °C for the sample composed of 50% acrylic and 50% wool (Figure 8) features signals related to pyrolysis products derived from both components. In particular, methacrylonitrile, 2,4-pentadienenitrile, 2-methylene-pentanedinitrile, and the four acrylonitrile trimers (AAA_1, AAA_2, AAA_3, AAA_4) are pyrolytic markers of acrylic fibers, while the presence of DKPs (cyclo(Pro-Ala), diketopyrrole and cyclo(Pro-Val)1&2) accounts for the animal fibers in the blend. Peaks identification is reported in Table S5 in Supplementary data.

Regarding the sample composed of 60% polyester and 40% polyamide, although the pyrolytic markers of both components can be detected in the pyrogram at 410 °C (Figure 9a), the pyrogram at 600 °C **(**Figure 9b) is dominated by the pyrolysis products derived from the polyester fraction. In addition, the presence of ε-caprolactam and vinyl benzoate identifies the polyamide and polyester as nylon 6 and PET, respectively. Peaks identification is reported in Tables S6 and S7 in Supplementary data.

Despite the low percentage of polyamide in the blend, two pyrolysis markers (i.e., ε-caprolactam and N-(5-cyanopentyl)hex-5-enamide) can be detected in the shot at 400 °C of the sample composed of 92% acrylic and 8% polyamide (Figure 10a). On the contrary, the shot at 600 °C (Figure 10b) features all the identified pyrolysis markers of acrylic fibers. The presence of ε-caprolactam allows to identify the polyamide as nylon 6. Peaks identification is reported in Tables S8 and S9 in Supplementary data.

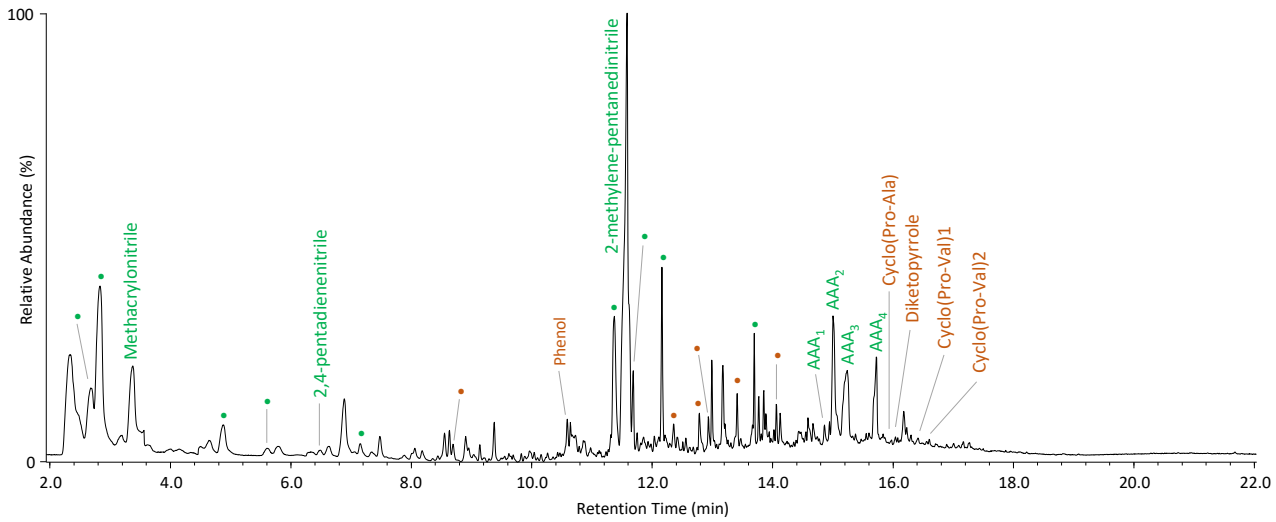

Figure 8: Py-GC/MS chromatogram obtained after pyrolysis at 600 °C of the sample composed of 50% acrylic and 50% wool. Peaks identification is reported in Table S5 in Supplementary data. The pyrolysis products derived from the acrylic fraction are highlighted in green while those derived from the wool fraction in brown.

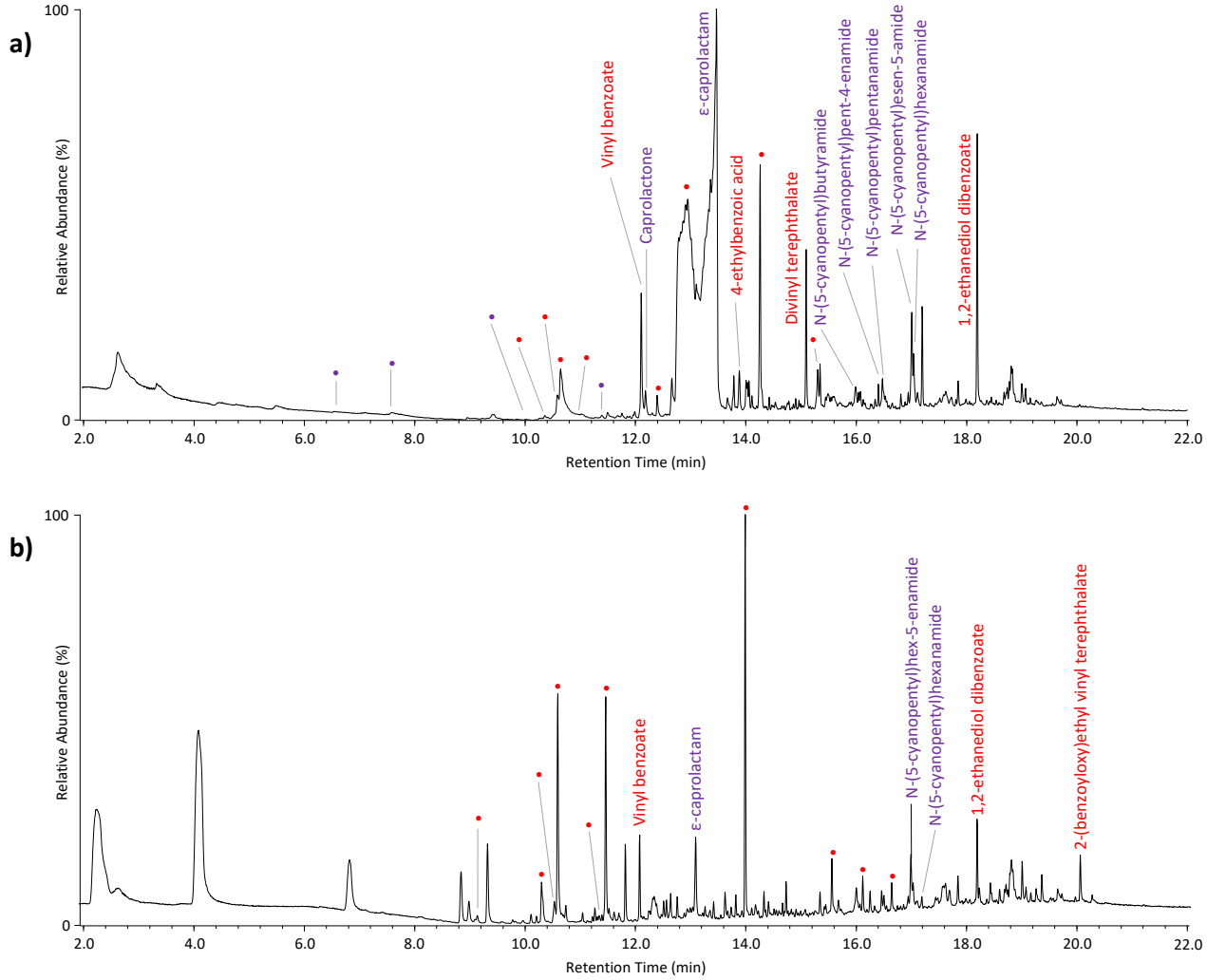

Figure 9: Py-GC/MS chromatograms obtained after pyrolysis at a) 410 °C and b) 600 °C of the sample composed of 60% polyester and 40% polyamide. Peaks identification is reported in Tables S6 and S7 in Supplementary data. The pyrolysis products derived from the polyester fraction are highlighted in red while those derived from the polyamide fraction in purple.

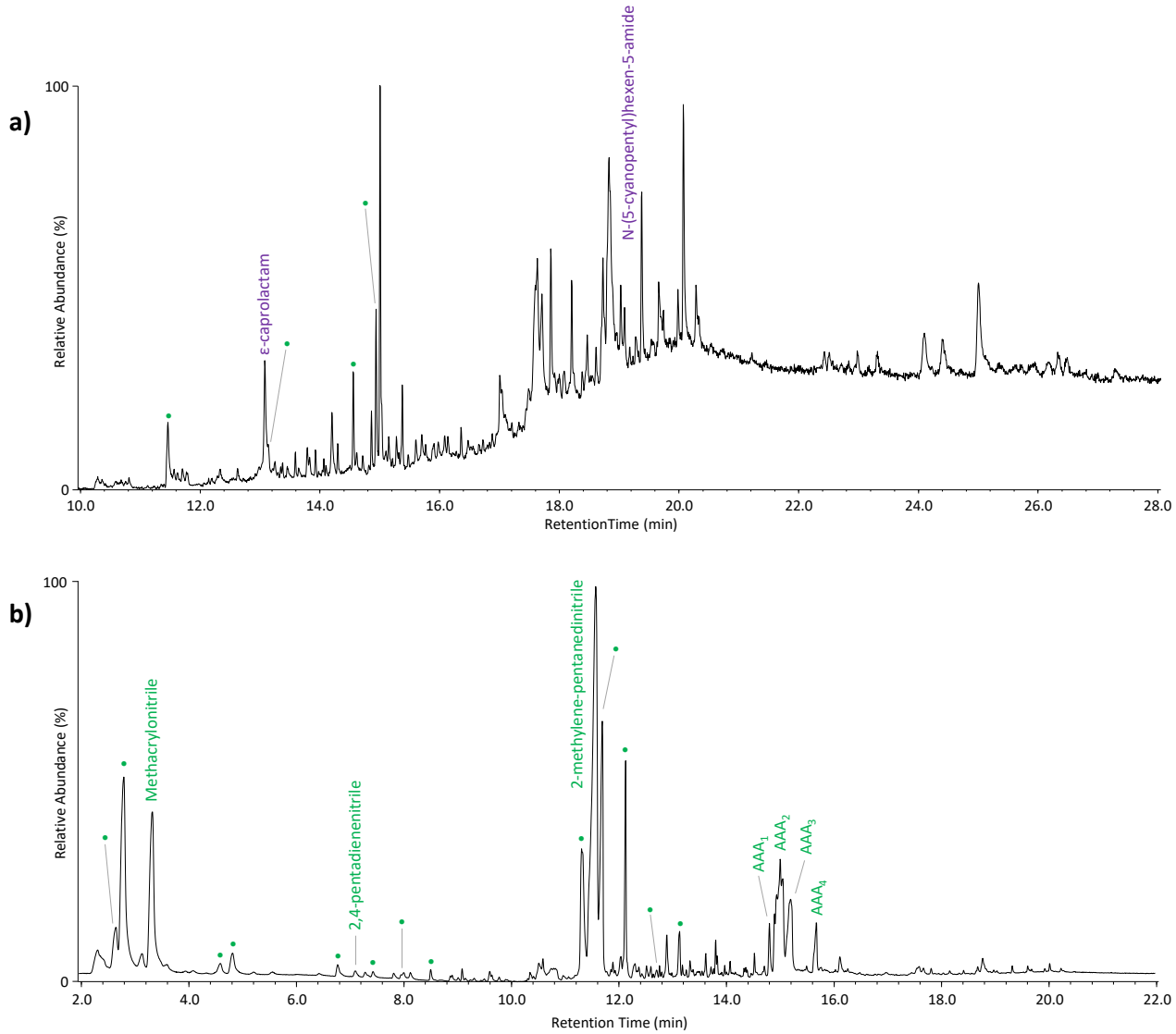

Figure 10: Py-GC/MS chromatograms obtained after pyrolysis at a) 400 °C and b) 600 °C of the sample composed of 92% acrylic and 8% polyamide. Peaks identification is reported in Tables S8 and S9 in Supplementary data. The pyrolysis products derived from the acrylic fraction are highlighted in green while those derived from the polyamide fraction in purple.

3.3 Historical samples

All historical samples were observed under visible transmitted light at 10x, 20x and 40x magnifications. The observed characteristics were compared with literature and reference samples to recognize the kind of fiber [69], [70]. The small size of the historical samples prevented ATR measurements from being performed. All samples were analyzed by Py-GC/MS. Samples A_02, A_04, and E_08 were not sufficiently abundant for both EGA-MS and pyrolysis to be performed, so they were only subjected to Py-GC/MS analysis. The results are discussed below.

3.3.1 Optical microscope (OM)

All the samples showed the characteristic morphological features of natural or artificial fibers.

Sample A_01 fibers were identified as cotton by the presence of ribbon-like twists with classical deconvolution on their structure. The appearance of sample A_02 fibers was characterized by the classical clarinet beak termination of silk fibers. The classification of sample A_03 is dubious because the fibers showed the typical striations of artificial fibers, but also the aspect of cotton with convolutions.

Fibers of samples E_01 and E_02 were smooth and without longitudinal striations or surface grooves, like silk fibers. In some areas the filaments appeared coupled two by two. These adhesions are due to the coagulation process and allow to recognize them as Bemberg fibers.

The remaining samples A_04, E_03, E_04, E_05, E_06, E_07, and E_08 showed a bright and striated surface in the direction of their axis, typical aspect of viscose and acetate fibers. Unfortunately, morphological evaluation was unable to discern between the two man-made fibers, so the identification must rely on other analytical approaches. Nonetheless, some consideration can be drawn from the OM observation: E_03 and E_06 showed a dotted surface maybe referable to a process of matte finish of viscose fibers, while samples A_04 and E_04 appeared very sheen and luster.

Representative OM images are reported in Figure 11 and the results of optical microscopical analyses are summarized in Table 4.

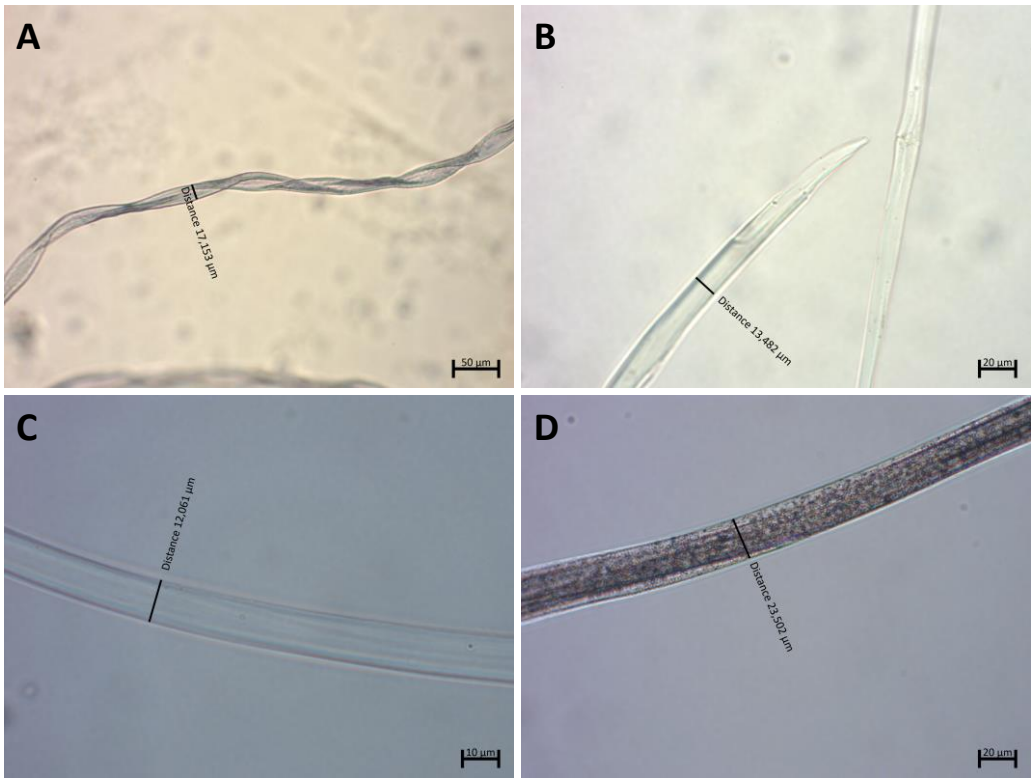

Figure 11: Fibers observed under visible transmitted light at different magnifications: sample A_01 at 10x magnification (A); sample A_02 at 20x magnification (B); sample E_02 at 40x magnification (C); sample E_03 at 20x magnification (D).

3.3.2 EGA-MS

Samples A_01, A_03, E_01, E_02, E_05, E_06, and E_07 showed similar TITs (Figure 12a). The average mass spectra obtained from the TITs (Figure 12b) are dominated by the characteristic ions of vegetal and regenerated fibers, in agreement with the OM results. Samples E_03 and E_04 presented a different TIT profile with a leading shoulder at temperatures below 350 °C (Figure 13a). The corresponding average mass spectra obtained from the TITs of samples E_03 and E_04 (Figure 13b) resemble those of acetate reference samples.

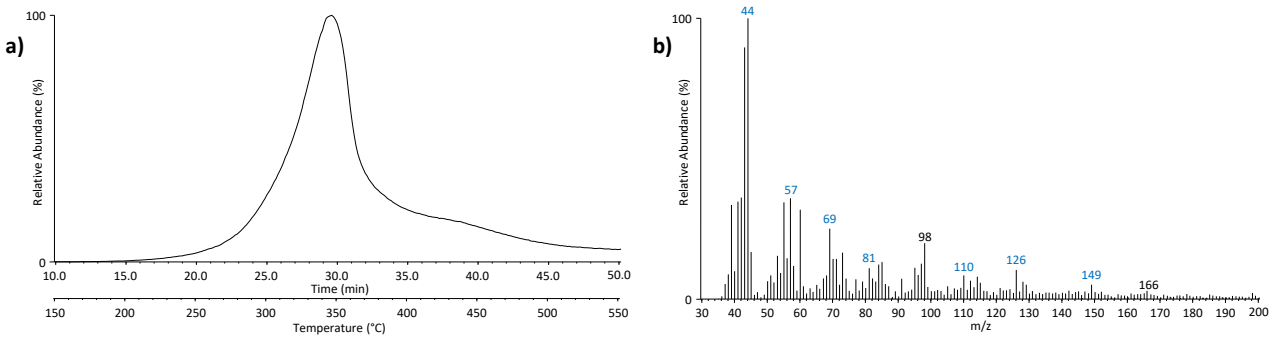

Figure 12: a) TIT of the sample A_01; b) Corresponding average mass spectrum obtained from the TIT (10-50 min, 150-550 °C). The characteristic ions of vegetal and regenerated fibers are highlighted in blue.

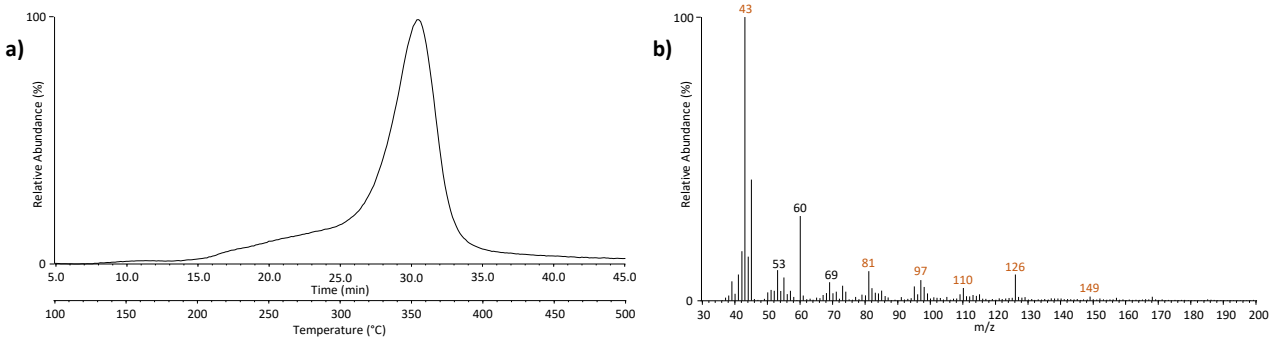

Figure 13: a) TIT of samples E_03; b) Corresponding average mass spectrum obtained from the TIT (5-45 min, 100-500 °C). The characteristic ions of acetate and Bemberg fibers are highlighted in brown.

3.3.3 Py-GC/MS

The pyrolytic profiles of samples A_01, A_03, E_01, E_02, E_05, E_06, E_07, and E_08 were similar. The levoglucosan peak in the pyrolytic profile of sample E_07 (Figure 14a) confirms the cellulose structure of the fibers, in agreement with OM and EGA-MS results. However, it was not possible to unambiguously identity the fiber type from the interpretation of the Py-GC/MS chromatogram. Samples A_04, E_03, and E_04 showed similar pyrograms. The broad acetic acid peak in the pyrolytic profile of sample E_03 (Figure 14b) and the detection of acetylated anhydrosugars identified the fibers as acetate. These results are in agreement with those obtained by EGA-MS and allow to deepen the identification performed by OM. The pyrolytic profile of A_02 sample (Figure 14c) is quite different from the other ones. The detection of phenol, 4-methyl-phenol, and DKPs points to the animal origin of the fiber, consistently with OM observation, but it was not possible to formulate more specific hypotheses based on the pyrogram. Peaks identification of each sample is reported in Tables S3, S10, and S11 in Supplementary data. All the materials constituting the microsamples were identified by combining the information achieved by OM and thermoanalytical techniques, as summarized in Table 4.

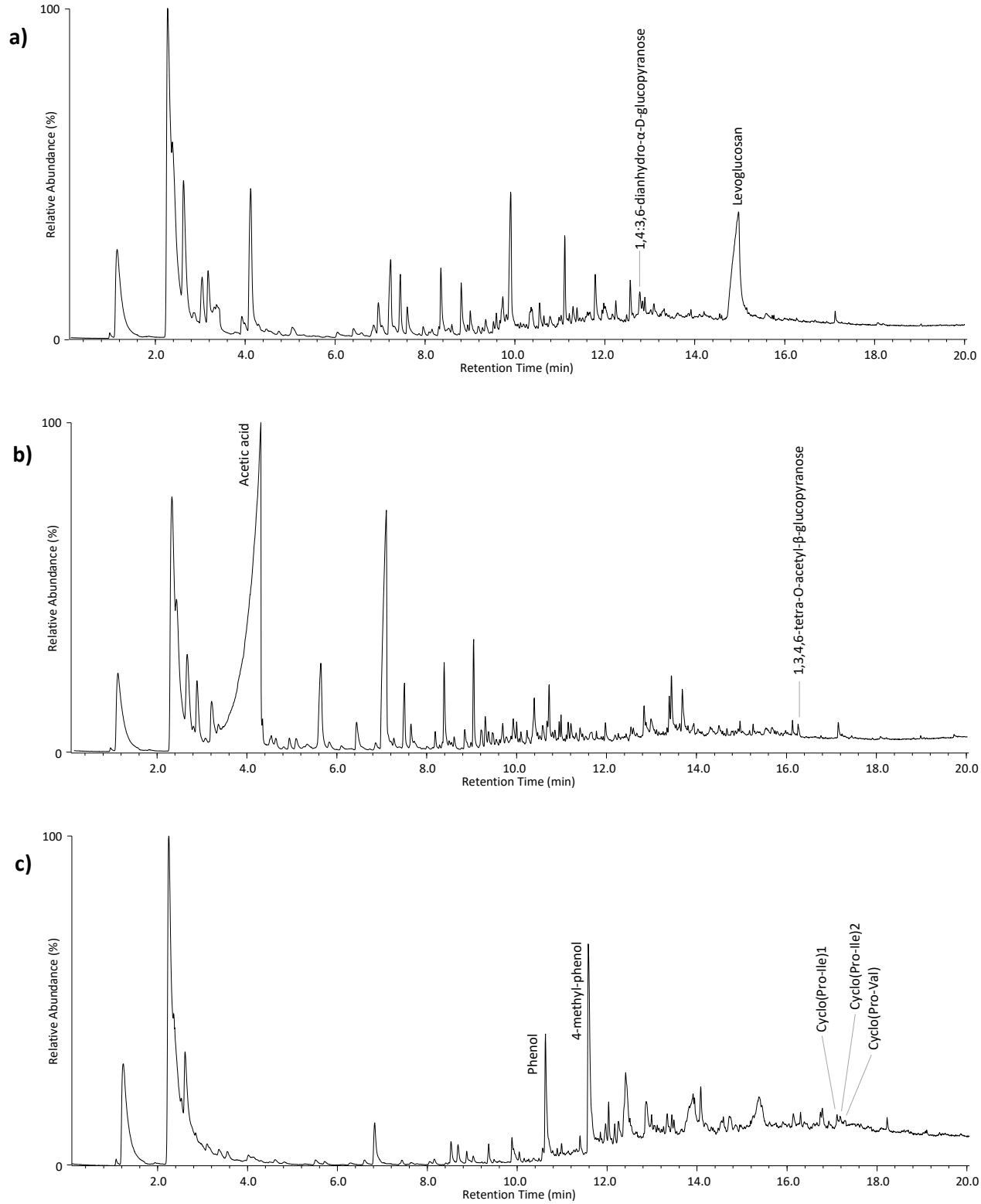

Figure 14: Py-GC/MS chromatograms obtained at 600 °C of samples a) E_07, b) E_03, and c) A_02. Peaks identification is reported in Tables S3, S10, and S11 in Supplementary data.

Table 4: Attribution of the constituting material of the unknown samples from the stage costumes.

Sample	Origin	Optical Microscopy	EGA-MS and Py-GC/MS	Final hypothesis
A_01	Arturo's jacket	Cotton	Cellulose fiber	Cotton
A_02	Arturo's jacket	Silk	Animal fiber	Silk

A_03	Arturo's cloak	Cotton (?)	Cellulose fiber	Cellulose fiber, probably cotton
A_04	Arturo's cloak	Viscose or acetate	Acetate	Acetate
E_01	Elvira's over skirt and bodice	Bemberg	Cellulose fiber	Bemberg
E_02	Elvira's over skirt and bodice	Bemberg	Cellulose fiber	Bemberg
E_03	Elvira's stomacher	Viscose or acetate	Acetate	Acetate
E_04	Elvira's skirt	Viscose or acetate	Acetate	Acetate
E_05	Elvira's train	Viscose or acetate	Cellulose fiber	Viscose
E_06	Elvira's train	Viscose or acetate	Cellulose fiber	Viscose
E_07	Elvira's petticoat	Viscose or acetate	Cellulose fiber	Viscose
E_08	Elvira's bodice	Viscose or acetate	Cellulose fiber	Viscose

4. Conclusions

A set including the most common natural and man-made textile fibers was analyzed by ATR-FTIR, and a database was created by EGA-MS and Py-GC/MS. These two thermo-analytical techniques are not being widely employed in the routine analyses of natural and artificial textile fibers, due in part to their recent development and the challenging interpretation of the results, especially when dealing with fibers.

The TITs acquired by EGA-MS of the pure samples allowed to discriminate each class of fibers based on their T_p. Some characteristic m/z ions have also been identified, as listed in Table 2. For the first time, a detailed pyrolysis database of natural and man-made fibers was developed, evidencing possible pyrolysis markers, and including different varieties of fibers for comparison (Table 2). All vegetal and regenerated fibers presented the characteristic peaks of 1,4:3,6-dianhydro-α-D-glucopyranose and levoglucosan in their pyrolytic profiles, with the notable exception of acetate. The latter was the only artificial fiber to show a characteristic, very broad, and intense acetic acid peak and a second peak related to 1,3,4,6-tetra-O-acetyl-β-D-glucopyranose. Unfortunately, no specific unique pyrolysis markers have been detected for natural and regenerated fibers, so Py-GC/MS can only point to the general composition of cellulose fibers, whereas the identification should also be guided by microscopy observation. Similarly, animal fibers can only be pointed out as a class by the detection of phenol, 4-methyl-phenol and DKPs in the Py-GC/MS chromatogram, but cannot be identified.

The analysis of three different samples of cotton, viscose and polyester fibers highlighted the major variability in the EGA and pyrolytic profiles of cotton, as expected for a natural fiber.

Three textile blends of known composition were then analyzed by ATR-FTIR, EGA-MS and Py-GC/MS to test the capability of each technique to discriminate and correctly identify both the components. Regarding the samples composed of 60% polyester and 40% polyamide, and 92% acrylic and 8% polyamide, ATR-FTIR failed to discriminate the polyamide fraction. The sensitivity of EGA-MS was insufficient to detect the polyamide fraction in the sample composed of 92% acrylic and 8% polyamide, due to its low concentration. However, the higher sensitivity of Py-GC/MS allowed to discriminate each component in every sample, confirming pyrolysis as a useful technique for a reliable and complete characterization of unknown textile samples.

The information obtained from the reference materials was applied to successfully investigate twelve microsamples collected from the stage costumes of the lyrical opera “I Puritani” directed by Franco Zeffirelli by optical microscopy, EGA-MS and Py-GC/MS. Despite the small sample size which enabled the use of ATR technique, the results highlighted the presence of cellulose in most samples, of acetate fibers in three samples, and of proteins in only one sample. In general, optical microscopy allowed a better discrimination of natural and artificial fibers compared to EGA-MS and Py-GC/MS, but showed poor capacity to distinguish between viscose and acetate fibers. On the contrary, EGA-MS and Py-GC/MS easily identified the uncertain fibers as acetate, proving a useful tool for the investigation of textile fibers.

Acknowledgments

The authors would like to thank the Università degli Studi di Palermo and the Teatro Massimo (Palermo, Italy), for involving us in the diagnostic campaign on the stage costumes. Antonella Manariti (Department of Chemistry and Industrial Chemistry of the Università di Pisa) is acknowledged for her assistance in the acquisition of the ATR-FTIR spectra.

Pisa University is also acknowledged for partially funding the research (project “PRA 2018 26”: Advanced analytical pyrolysis to study polymers in renewable energy, environment, cultural heritage - 2018-2020) and the Centre for Instrument Sharing of the University of Pisa (CISUP) for providing the pyrolysis instrumentation.

Bibliography

[1] M. M. Houck, “Ways of identifying textile fibers and materials,” in *Identification of textile fibers*, 1st ed., M. M. Houck, Ed. Cambridge: Woodhead Publishing, 2009, pp. 6–26.

[2] J. W. S. Hearle, “Fibre structure: its formation and relation to performance,” in *Handbook of textile fibre structure*, 1st ed., vol. 1, S. J. Eichhorn, J. W. S. Hearle, M. Jaffe, and T. Kikutani, Eds. Cambridge: Woodhead Publishing, 2009, pp. 3–21.

[3] C. Tan, H. Chen, Z. Lin, and T. Wu, “Category identification of textile fibers based on near-infrared spectroscopy combined with data description algorithms,” *Vib Spectrosc*, vol. 100, pp. 71–78, Jan. 2019, doi: 10.1016/J.VIBSPEC.2018.11.004.

[4] R. Sinclair, Ed., *Textiles and fashion*, 1st ed. Cambridge: Woodhead Publishing, 2015.

[5] F. Zapata, F. E. Ortega-Ojeda, and C. García-Ruiz, “Forensic examination of textile fibres using Raman imaging and multivariate analysis,” *Spectrochimica Acta Part A: Molecular and Biomolecular Spectroscopy*, vol. 268, p. 120695, Mar. 2022, doi: 10.1016/J.SAA.2021.120695.

[6] L. de Palaminy, C. Daher, and C. Moulherat, “Development of a non-destructive methodology using ATR-FTIR and chemometrics to discriminate wild silk species in heritage collections,” *Spectrochimica Acta Part A: Molecular and Biomolecular Spectroscopy*, vol. 270, p. 120788, Apr. 2022, doi: 10.1016/J.SAA.2021.120788.

[7] J. Gago, O. Carretero, A. v. Filgueiras, and L. Viñas, “Synthetic microfibers in the marine environment: A review on their occurrence in seawater and sediments,” *Marine Pollution Bulletin*, vol. 127. Elsevier Ltd, pp. 365–376, Feb. 01, 2018. doi: 10.1016/j.marpolbul.2017.11.070.

[8] A. Rebelein, I. Int-Veen, U. Kammann, and J. P. Scharsack, “Microplastic fibers — Underestimated threat to aquatic organisms?,” *Science of the Total Environment*, vol. 777. Elsevier B.V., Jul. 10, 2021. doi: 10.1016/j.scitotenv.2021.146045.

[9] S. T. L. Sait *et al.*, “Microplastic fibres from synthetic textiles: Environmental degradation and additive chemical content,” *Environmental Pollution*, vol. 268, p. 115745, Jan. 2021, doi: 10.1016/J.ENVPOL.2020.115745.

[10] T. Stanton, M. Johnson, P. Nathanail, W. MacNaughtan, and R. L. Gomes, “Freshwater and airborne textile fibre populations are dominated by ‘natural’, not microplastic, fibres,” *Science of The Total Environment*, vol. 666, pp. 377–389, May 2019, doi: 10.1016/J.SCITOTENV.2019.02.278.

[11] M. Wilding, “Optical microscopy for textile fibre identification,” in *Identification of textile fibers*, 1st ed., M. M. Houck, Ed. Cambridge: Woodhead Publishing, 2009, pp. 133–157.

[12] M. Houck, “Textiles,” in *Forensic chemistry: fundamentals and applications*, 1st ed., J. Siegel, Ed. New Jersey: Blackwell Pub, 2015, pp. 40–74.

[13] F. Coletti, M. Romani, G. Ceres, U. Zammit, and M. C. Guidi, “Evaluation of microscopy techniques and ATR-FTIR spectroscopy on textile fibers from the Vesuvian area: A pilot study on degradation processes that prevent the characterization of bast fibers,” *Journal of Archaeological Science: Reports*, vol. 36, p. 102794, Apr. 2021, doi: 10.1016/J.JASREP.2021.102794.

[14] C. Bergfjord and B. Holst, “A procedure for identifying textile bast fibres using microscopy: Flax, nettle/ramie, hemp and jute,” *Ultramicroscopy*, vol. 110, no. 9, pp. 1192–1197, Aug. 2010, doi: 10.1016/J.ULTRAMIC.2010.04.014.

[15] M. Gleba, “From textiles to sheep: investigating wool fibre development in pre-Roman Italy using scanning electron microscopy (SEM),” *Journal of Archaeological Science*, vol. 39, no. 12, pp. 3643–3661, Dec. 2012, doi: 10.1016/J.JAS.2012.06.021.

[16] E. Karpova, V. Vasiliev, V. Mamatyuk, N. Polosmak, and L. Kundo, “Xiongnu burial complex: A study of ancient textiles from the 22nd Noin-Ula barrow (Mongolia, first century AD),” *Journal of Archaeological Science*, vol. 70, pp. 15–22, Jun. 2016, doi: 10.1016/j.jas.2016.04.001.

[17] H. Zhao, J. H. Kwak, Z. Conrad Zhang, H. M. Brown, B. W. Arey, and J. E. Holladay, “Studying cellulose fiber structure by SEM, XRD, NMR and acid hydrolysis,” *Carbohydrate Polymers*, vol. 68, no. 2, pp. 235–241, Mar. 2007, doi: 10.1016/j.carbpol.2006.12.013.

[18] I. Karapanagiotis, D. Mantzouris, P. Kamaterou, D. Lampakis, and C. Panayiotou, “Identification of materials in post-Byzantine textiles from Mount Athos,” *Journal of Archaeological Science*, vol. 38, no. 12, pp. 3217–3223, 2011, doi: 10.1016/j.jas.2011.06.022.

[19] R. Powell, P. Collins, G. Horsley, J. Coumbaros, and W. van Bronswijk, “Enhancing the evidential value of textile fibres Part 2: Application of a database-driven fibre comparison strategy to a cold-case investigation,” *Forensic Science International*, vol. 325, p. 110894, Aug. 2021, doi: 10.1016/J.FORSCIINT.2021.110894.

[20] A. Götz, V. Senz, W. Schmidt, J. Huling, N. Grabow, and S. Illner, “General image fiber tool: A concept for automated evaluation of fiber diameters in SEM images,” *Measurement*, vol. 177, p. 109265, Jun. 2021, doi: 10.1016/J.MEASUREMENT.2021.109265.

[21] C. M. Hussain, D. Rawtani, G. Pandey, and M. Tharmavaram, “Optical microscopy for forensic samples,” *Handbook of Analytical Techniques for Forensic Samples*, pp. 213–234, Jan. 2021, doi: 10.1016/B978-0-12-822300-0.00012-4.

[22] S. Farah, T. Tsach, A. Bentolila, and A. J. Domb, “Morphological, spectral and chromatography analysis and forensic comparison of PET fibers,” *Talanta*, vol. 123, pp. 54–62, Jun. 2014, doi: 10.1016/J.TALANTA.2014.01.041.

[23] C. Besnard *et al.*, “Analysis of in vitro demineralised human enamel using multi-scale correlative optical and scanning electron microscopy, and high-resolution synchrotron wide-angle X-ray scattering,” *Materials & Design*, vol. 206, p. 109739, Aug. 2021, doi: 10.1016/J.MATDES.2021.109739.

[24] R. Maddipatla and P. Tankam, “Development of high-speed, integrated high-resolution optical coherence microscopy and dual-channel fluorescence microscopy for the simultaneous co-registration of reflectance and fluorescence signals,” *Optics and Lasers in Engineering*, vol. 149, p. 106823, Feb. 2022, doi: 10.1016/J.OPTLASENG.2021.106823.

[25] Y. Bai, W. Ngo, S. Khanal, and J. J. Nichols, “Characterization of the thickness of the Tear Film Lipid Layer in Meibomian Gland Dysfunction using high resolution optical microscopy,” *The Ocular Surface*, vol. 24, pp. 34–39, Apr. 2022, doi: 10.1016/J.JTOS.2021.12.011.

[26] P. H. Greaves, “Alternative and specialised textile fibre identification tests,” in *Identification of textile fibers*, 1st ed., M. M. Houck, Ed. Cambridge: Woodhead Publishing, 2009, pp. 181–202.

[27] R. Powell, W. van Bronswijk, and J. Coumbaros, “Enhancing the evidential value of textile fibres: Part 1: Development of a spectral database and evaluative comparison strategy,” *Forensic Science International*, vol. 287, pp. 54–62, Jun. 2018, doi: 10.1016/J.FORSCIINT.2018.03.025.

[28] J. M. Home and R. J. Dudley, “A Summary of Data Obtained from a Collection of Fibres from Casework Materials,” *Journal of the Forensic Science Society*, vol. 20, no. 4, pp. 253–261, Oct. 1980, doi: 10.1016/S0015-7368(80)71352-X.

[29] N. Ferrer, “Forensic Science, Applications of Infrared Spectroscopy,” *Reference Module in Chemistry, Molecular Sciences and Chemical Engineering*, Jan. 2014, doi: 10.1016/B978-0-12-409547-2.10998-9.

[30] N. Ferrer, “Forensic Science, Applications of IR Spectroscopy,” *Encyclopedia of Spectroscopy and Spectrometry*, pp. 695–706, Jan. 2017, doi: 10.1016/B978-0-12-803224-4.00151-5.

[31] T. A. Joslin Yogi, M. Penrod, M. Holt, and P. Buzzini, “The relationship between cross-sectional shapes and FTIR profiles in synthetic wig fibers and their discriminating abilities — An evidential value perspective,” *Forensic Science International*, vol. 283, pp. 94–102, Feb. 2018, doi: 10.1016/j.forsciint.2017.12.015.

[32] F. Zapata, F. E. Ortega-Ojeda, and C. García-Ruiz, “Forensic examination of textile fibres using Raman imaging and multivariate analysis,” *Spectrochimica Acta Part A: Molecular and Biomolecular Spectroscopy*, vol. 268, p. 120695, Mar. 2022, doi: 10.1016/J.SAA.2021.120695.

[33] L. Lepot, K. de Wael, F. Gason, and B. Gilbert, “Application of Raman spectroscopy to forensic fibre cases,” *Science & Justice*, vol. 48, no. 3, pp. 109–117, Sep. 2008, doi: 10.1016/J.SCIJUS.2007.09.013.

[34] L. Lepot, K. Lunstroot, and K. de Wael, “Interpol review of fibres and textiles 2016–2019,” *Forensic Science International: Synergy*, vol. 2, pp. 481–488, Jan. 2020, doi: 10.1016/J.FSISYN.2020.01.014.

[35] P. P. Meleiro and C. Garciá-Ruiz, “Spectroscopic techniques for the forensic analysis of textile fibers,” *Applied Spectroscopy Reviews*, vol. 51, no. 4, pp. 258–281, Apr. 2016, doi: 10.1080/05704928.2015.1132720.

[36] V. Causin, C. Marega, S. Schiavone, and A. Marigo, “A quantitative differentiation method for acrylic fibers by infrared spectroscopy,” *Forensic Science International*, vol. 151, no. 2–3, pp. 125–131, Jul. 2005, doi: 10.1016/j.forsciint.2005.02.004.

[37] M. C. Grieve, “Another look at the classification of acrylic fibres, using FTIR microscopy,” *Science and Justice - Journal of the Forensic Science Society*, vol. 35, no. 3, pp. 179–190, 1995, doi: 10.1016/S1355-0306(95)72659-4.

[38] P. Peets, I. Leito, J. Pelt, and S. Vahur, “Identification and classification of textile fibres using ATR-FT-IR spectroscopy with chemometric methods,” *Spectrochimica Acta - Part A: Molecular and Biomolecular Spectroscopy*, vol. 173, pp. 175–181, Feb. 2017, doi: 10.1016/j.saa.2016.09.007.

[39] G. Jochem and R. J. Lehnert, “On the potential of Raman microscopy for the forensic analysis of coloured textile fibres,” *Science and Justice - Journal of the Forensic Science Society*, vol. 42, no. 4, pp. 215–221, 2002, doi: 10.1016/S1355-0306(02)71831-5.

[40] J. v. Miller and E. G. Bartick, “Forensic analysis of single fibers by Raman spectroscopy,” *Applied Spectroscopy*, vol. 55, no. 12, pp. 1729–1732, Dec. 2001, doi: 10.1366/0003702011954099.

[41] A. L. Lusher, A. Burke, I. O’Connor, and R. Officer, “Microplastic pollution in the Northeast Atlantic Ocean: Validated and opportunistic sampling,” *Marine Pollution Bulletin*, vol. 88, no. 1–2, pp. 325–333, Nov. 2014, doi: 10.1016/J.MARPOLBUL.2014.08.023.

[42] I. Peeken *et al.*, “Arctic sea ice is an important temporal sink and means of transport for microplastic,” *Nature Communications*, vol. 9, no. 1, Dec. 2018, doi: 10.1038/s41467-018-03825-5.

[43] I. vanden Berghe, “Towards an early warning system for oxidative degradation of protein fibres in historical tapestries by means of calibrated amino acid analysis,” *Journal of Archaeological Science*, vol. 39, no. 5, pp. 1349–1359, 2012, doi: 10.1016/j.jas.2011.12.033.

[44] T. G. Schotman, X. Xu, N. Rodewijk, and J. van der Weerd, “Application of dye analysis in forensic fibre and textile examination: Case examples,” *Forensic Science International*, vol. 278, pp. 338–350, Sep. 2017, doi: 10.1016/j.forsciint.2017.07.026.

[45] K. de Wael, K. van Dijck, and F. Gason, “Discrimination of reactively-dyed cotton fibres with thin layer chromatography and UV microspectrophotometry,” *Science & Justice*, vol. 55, no. 6, pp. 422–430, Dec. 2015, doi: 10.1016/J.SCIJUS.2015.06.001.

[46] A. Kramell *et al.*, “Dyes of late Bronze Age textile clothes and accessories from the Yanghai archaeological site, Turfan, China: Determination of the fibers, color analysis and dating,” *Quaternary International*, vol. 348, pp. 214–223, Oct. 2014, doi: 10.1016/j.quaint.2014.05.012.

[47] D. Tamburini, “Investigating Asian colourants in Chinese textiles from Dunhuang (7th-10th century AD) by high performance liquid chromatography tandem mass spectrometry – Towards the creation of a mass spectra database,” *Dyes and Pigments*, vol. 163, pp. 454–474, Apr. 2019, doi: 10.1016/j.dyepig.2018.12.025.

[48] C. Hu *et al.*, “A sensitive HPLC-MS/MS method for the analysis of fiber dyes,” *Forensic Chemistry*, vol. 11, pp. 1–6, Dec. 2018, doi: 10.1016/j.forc.2018.08.001.

[49] F. Sabatini, T. Nacci, I. Degano, and M. P. Colombini, “Investigating the composition and degradation of wool through EGA/MS and Py-GC/MS,” *Journal of Analytical and Applied Pyrolysis*, vol. 135, pp. 111–121, Oct. 2018, doi: 10.1016/J.JAAP.2018.09.012.

[50] F. Sabatini *et al.*, “On the set of fellini’s movies: Investigating and preserving multi-material stage costumes exploiting spectroscopic and mass spectrometric techniques,” *Applied Sciences (Switzerland)*, vol. 11, no. 7, Apr. 2021, doi: 10.3390/app11072954.

[51] S. O’Brien *et al.*, “Airborne emissions of microplastic fibres from domestic laundry dryers,” *Science of The Total Environment*, vol. 747, p. 141175, Dec. 2020, doi: 10.1016/J.SCITOTENV.2020.141175.

[52] P. Zhu, S. Sui, B. Wang, K. Sun, and G. Sun, “A study of pyrolysis and pyrolysis products of flame-retardant cotton fabrics by DSC, TGA, and PY–GC–MS,” *Journal of Analytical and Applied Pyrolysis*, vol. 71, no. 2, pp. 645–655, Jun. 2004, doi: 10.1016/J.JAAP.2003.09.005.

[53] J. la Nasa, G. Biale, D. Fabbri, and F. Modugno, “A review on challenges and developments of analytical pyrolysis and other thermoanalytical techniques for the quali-quantitative determination of microplastics,” *Journal of Analytical and Applied Pyrolysis*, vol. 149. Elsevier, p. 104841, Aug. 01, 2020. doi: 10.1016/j.jaap.2020.104841.

[54] C. Cirrincione, “I costumi teatrali e il riuso nel passato e nel futuro: creazione di un protocollo d’uso e contributo alla definizione della scheda VAC-S,” Palermo, 2012.

[55] F. Sabatini, I. Degano, and M. van Bommel, “Investigating the in-solution photodegradation pathway of Diamond Green G by chromatography and mass spectrometry,” *Coloration Technology*, vol. 137, no. 5, pp. 456–467, Oct. 2021, doi: 10.1111/cote.12538.

[56] A. G. Wilkes, “The viscose process,” in *Regenerated cellulose fibres*, 1st ed., C. Woodings, Ed. Cambridge: Woodhead Publishing, 2001, pp. 37–61.

[57] S. Tsuge, H. Ohtani, and C. Watanabe, *Pyrolysis-GC/MS data book of synthetic polymers. Pyrograms, thermograves and MS of pyrolyzates.*, 1st ed. Oxford: Elsevier, 2011.

[58] Y. Wang, A. Akbarzadeh, L. Chong, J. Du, N. Tahir, and M. K. Awasthi, "Catalytic pyrolysis of lignocellulosic biomass for bio-oil production: A review," *Chemosphere*, vol. 297, p. 134181, Jun. 2022, doi: 10.1016/J.CHEMOSPHERE.2022.134181.

[59] Q. Lu, X. C. Yang, C. Q. Dong, Z. F. Zhang, X. M. Zhang, and X. F. Zhu, "Influence of pyrolysis temperature and time on the cellulose fast pyrolysis products: Analytical Py-GC/MS study," *Journal of Analytical and Applied Pyrolysis*, vol. 92, no. 2, pp. 430–438, Nov. 2011, doi: 10.1016/J.JAAP.2011.08.006.

[60] S. Orsini, F. Parlanti, and I. Bonaduce, "Analytical pyrolysis of proteins in samples from artistic and archaeological objects," *Journal of Analytical and Applied Pyrolysis*, vol. 124, pp. 643–657, Mar. 2017, doi: 10.1016/J.JAAP.2016.12.017.

[61] S. v Levchik, E. D. Weil, and M. Lewin, "Thermal decomposition of aliphatic nylons," *Polymer International*, vol. 48, pp. 532–557, 1999.

[62] P. Yin, H. Chen, X. Liu, Q. Wang, Y. Jiang, and R. Pan, "Mass Spectral Fragmentation Pathways of Phthalate Esters by Gas Chromatography-Tandem Mass Spectrometry," *Analytical Letters*, vol. 47, no. 9, pp. 1579–1588, 2014, doi: 10.1080/00032719.2013.879658.

[63] S. Mishra, C. charan Rath, and A. P. Das, "Marine microfiber pollution: A review on present status and future challenges," *Marine Pollution Bulletin*, vol. 140, pp. 188–197, Mar. 2019, doi: 10.1016/J.MARPOLBUL.2019.01.039.

[64] M. P. Ansell and L. Y. Mwaikambo, "The structure of cotton and other plant fibres," in *Handbook of textile fibres structure*, 1st ed., vol. 2, S. J. Eichhorn, S. W. J. Hearle, M. Jaffe, and T. Kikutani, Eds. Cambridge: Woodhead Publishing, 2009, pp. 62–94.

[65] Frontier Lab, "F-Search System Ver. 3.6," Sep. 25, 2021. https://www.frontier-lab.com/products/multi-functional-pyrolysis-system/17821/ (accessed Feb. 14, 2022).

[66] G. Dierkes, T. Lauschke, S. Becher, H. Schumacher, C. Földi, and T. Ternes, "Quantification of microplastics in environmental samples via pressurized liquid extraction and pyrolysis-gas chromatography," *Analytical and Bioanalytical Chemistry*, vol. 411, no. 26, pp. 6959–6968, Oct. 2019, doi: 10.1007/s00216-019-02066-9.

[67] B. J. Holland and J. N. Hay, "The thermal degradation of poly(vinyl alcohol)," *Polymer (Guildf)*, vol. 42, no. 16, pp. 6775–6783, Jul. 2001, doi: 10.1016/S0032-3861(01)00166-5.

[68] F. Nardella, S. Bellavia, M. Mattonai, and E. Ribechini, "Co-pyrolysis of wood and plastic: Evaluation of synergistic effects and kinetic data by evolved gas analysis-mass spectrometry (EGA-MS)," *Journal of Analytical and Applied Pyrolysis*, vol. 159, p. 105308, Oct. 2021, doi: 10.1016/J.JAAP.2021.105308.

[69] I. Markova, "Regenerated cellulosic and protein fibers," in *Textile fiber microscopy. A practical approach*, 1st ed., I. Markova, Ed. Wiley, 2019, pp. 101–122.

[70] C. Quaglierini, "Fibre tessili artificiali," in *Chimica delle fibre tessili*, C. Quaglierini, Ed. Zanichelli, 1989, pp. 146–173.